SELF-CONSISTENT STOCHASTIC ELECTRON HEATING IN RADIO FREQUENCY DISCHARGES

by

C. G. Goedde, A. J. Lichtenberg, and M. A. Lieberman

Memorandum No. UCB/ERL M88/29

9 May 1988

SELF-CONSISTENT STOCHASTIC ELECTRON HEATING IN RADIO FREQUENCY DISCHARGES

by

C. G. Goedde, A. J. Lichtenberg, and M. A. Lieberman

Memorandum No. UCB/ERL M88/29

9 May 1988

ELECTRONICS RESEARCH LABORATORY

College of Engineering
University of California, Berkeley
94720

SELF-CONSISTENT STOCHASTIC ELECTRON HEATING IN RADIO FREQUENCY DISCHARGES

by

C. G. Goedde, A. J. Lichtenberg, and M. A. Lieberman

Memorandum No. UCB/ERL M88/29

9 May 1988

ELECTRONICS RESEARCH LABORATORY

College of Engineering
University of California, Berkeley
94720

Self-Consistent Stochastic Electron Heating in Radio Frequency Discharges

C. G. Goedde
Department of Physics
University of California, Berkeley, CA 94720

A. J. Lichtenberg
and
M. A. Lieberman
Department of Electrical Engineering and Computer Sciences
and the Electronics Research Laboratory
University of California, Berkeley, CA 94720

ABSTRACT

Fermi acceleration is considered as an underlying mechanism for electron heating in r.f. discharges, in which the heating arises from the reflection of electrons from moving sheaths. By examining the dynamics of the electron collisions with the sheaths, the map that describes the electron motion is derived. For high frequency discharges ($\omega/2\pi > 50$ MHz), the electron motion is shown to be stochastic. By combining these dynamics with collisional effects in the bulk plasma and incorporating self-consistent physical constraints, a self-consistent model of the discharge is developed. The model is used to calculate physically interesting quantities, such as the electron temperature and average lifetime, and to predict the minimum pressure necessary to sustain the plasma. The distribution of electron energies is shown to be non-Maxwellian. These results can be applied to experimentally interesting parallel plate r.f. plasma discharges to predict the operating conditions necessary for stochastic heating to occur.

1. Introduction

In this paper we consider the heating of electrons in a radio frequency discharge by high-field, oscillating sheaths. This mechanism, which can be more important than energy transfer in the bulk plasma, has been explored by Godyak and colleagues [1–5], and by Akhiezer and Bakai [6,7]. In these treatments the underlying mechanism for the heating is Fermi acceleration, with the energy change arising from the reflection of the electron from a moving sheath [8–11].

It is well known [9–11] that the Fermi acceleration mechanism does not always produce continuous heating, but may, depending on the parameters, lead either to regular oscillations or to stochastic heating. The transition between the two constitutes an energy barrier to the heating of particles. For the purpose of calculating heating rates, Godyak *et al* and Akhiezer and Bakai assumed the heating to be stochastic. Furthermore, the sheath was treated in its simplest approximation as an impulsive reflector. As will be seen, the detailed sheath dynamics plays a profound role in determining the heating rates and the boundary between stochastic and regular motion.

The Fermi acceleration dynamics cannot be considered independently of the bulk plasma properties. The interaction between sheath and bulk plasma can be quite complicated and depends strongly on the background gas pressure. If the discharge can be operated at sufficiently low pressure that the electrons experience many sheath reflections before suffering an effective ninety degree collision, then the effects of ohmic heating in the plasma are negligible, and the primary effects of the collisional processes are the elastic scattering of electrons into the perpendicular directions and the ionization and exitation of neutrals.

In contrast, Godyak [2] treats both sheath and bulk heating, assuming that the collisional processes in the bulk plasma generate the usual ohmic heating and are additive to the sheath heating process.

The preceding effects can be treated in terms of a test particle interacting with known regular and statistical forces. The results are statistically summed over a distribution of test particles. In addition, there are a number of self-consistency conditions that must be met for an r.f. discharge. In particular, charge must be conserved, which sets the d.c. sheath potential and a minimum pressure required to sustain the discharge. The Bohm sheath condition and the Child-Langmuir law determine the sheath thickness. These constraints have been applied in the calculations of Godyak [2] to a more complicated geometry than the one dimensional system which is considered here. Godyak and Ganna [3] also introduce more plasma detail, such as plasma nonuniformities. However, the full complexity of the plasma-sheath combination, investigated in d.c. discharges [12], is not employed. In experimental investigations Popov and Godyak [5] show the general correctness of the notion that the interaction of the electrons with the plasma sheath can serve as the main source of energy transfer at low pressures, and Godyak and Oks [13] measure non-Maxwellian electron distributions in high frequency discharges. In these studies the simplified assumptions of the mechanism of sheath energy transfer were used, and the distribution of electron energy was not determined analytically.

The regime of interest is where the chaotic dynamics dominate the electron motion, which is the range of pressures in the near-collisionless regime where electrons experience many interactions with the sheaths before suffering collisions with neutrals. That is, the regime where $\tau_b \ll \tau_c$, where τ_b is the typical bounce time and τ_c is the mean time for electron

elastic collisions with neutrals. With this time ordering the electron motion is adequately described by the single particle dynamics. Additionally, if the electron lifetime, τ_l, and the effective time for energy losses due to ionization and excitation, τ_z, are large compared to these times, the electron velocity distribution will be isotropic and the ionization, while sufficient to maintain the discharge, will not result in significant electron energy loss. Thus, we are interested in the range of pressure where

$$\tau_b \ll \tau_c \ll \tau_l \lesssim \tau_z. \tag{1}$$

In this pressure range the main effects of collisions are phase randomization and an isotropization of the electron velocity distribution due to elastic scattering.

The purpose of this paper is to apply the methods of nonlinear dynamics to the interaction of electrons with the localized oscillating electric fields in a plasma sheath and to calculate the parameter regimes for which the resulting electron motion can be stochastic. By solving the equations of motion, an exact single particle mapping which can be iterated numerically is developed, as is an approximate model which can be used for analytic calculations. With the addition of the self-consistent treatment of the physical contraints, the model can be used to calculate physically interesting quantities, such as the electron temperature and average lifetime, and to predict the minimum pressure necessary to sustain the plasma. The distribution of electron energies can also be calculated. These results can be applied to experimentally interesting parallel plate r.f. plasma discharges to predict the operating conditions necessary for stochastic heating to occur.

2. Hamiltonian Dynamics

We consider is a plane-parallel r.f. plasma discharge operating at frequency ω, and begin by examining the dynamics in the collisionless limit. The discharge is modeled in one dimension by treating it as two distinct regions. The first region is the body of the plasma, of length l, which is taken to be field free. The second is the thin sheath region of thickness $s(t)$ and mean thickness s_0. The sheath thickness and the electric fields in the sheath region depend on the frequency, the d.c. voltage V_{dc} and the r.f. voltage amplitude V_{rf} between the plasma and the discharge plates. Using continuity of current and assuming that the electrons move as a body with respect to the r.f. field, then, if we ignore ion space charge in the sheath as a first approximation, the sheath electric field is a constant $E = V_{dc}/s_0$, and the sheath thickness follows the voltage as

$$s(t) \simeq s_0 \left[1 + \frac{V_{rf}}{V_{dc}} \cos(\omega t + \phi)\right]. \tag{2}$$

The equation of motion for an electron in the sheath is, trivially,

$$m_e \frac{d^2x}{dt^2} = -\frac{eV_{dc}}{s_0}.$$

It is convenient to introduce the dimensionless parameters α, β and ϵ:

$$\alpha = \frac{m_e \omega^2 s_0^2}{eV_{dc}}, \qquad \beta = \frac{V_{rf}}{V_{dc}}, \qquad \epsilon = \frac{s_0}{l},$$

and the dimensionless position δ and time τ:

$$\delta = \frac{x}{s_0}, \qquad \tau = \omega t.$$

In terms of these variables,

$$\frac{d^2\delta}{d\tau^2} = -\frac{1}{\alpha}. \tag{3}$$

Integrating (3) once gives the velocity of an electron as it moves through the sheath

$$\mu(\tau) = \mu(0) - \frac{\tau}{\alpha}, \tag{4}$$

where $\mu \equiv d\delta/d\tau$ is the dimensionless velocity. Integrating again gives the position of an electron as a function of time in the sheath:

$$\delta(\tau) - \delta(0) = -\frac{\tau^2}{2\alpha} + \mu(0)\tau. \tag{5a}$$

Here $\delta(0)$ and $\delta(\tau)$ are the positions of the sheath boundary when the electron enters and leaves the sheath, that is,

$$\begin{aligned} \delta(0) &= -\beta\cos\phi, \\ \delta(\tau) &= -\beta\cos(\tau+\phi). \end{aligned} \tag{5b}$$

Equation (5) is a transcendental equation for the electron transit time τ for a single pass through the sheath. Using this value of τ in (4) yields the change in velocity due to each interaction with the sheath. This model will yield a mapping that to lowest order becomes the simplified Fermi acceleration problem of a ball bouncing between a fixed and an oscillating wall [8–11].

We consider the motion to occur in two distinct parts, the unperturbed motion through the bulk plasma, where the electron velocity is constant, and the rapidly varying velocity region in the sheath. The combination of the two regions constitutes a mapping of the

velocity and phase of the motion between successive entries into the sheath region, labelled by integers n, $n+1$, *etc.* With $\mu(0) = \mu_n$ and $\mu(\tau) = -\mu_{n+1}$, (4) can be rewritten

$$\mu_{n+1} = -\mu_n + \frac{\tau}{\alpha}. \tag{6a}$$

If $\epsilon \ll 1$ then the zero order phase advance equation is

$$\phi_{n+1} = \phi_n + \frac{1}{\epsilon\mu_{n+1}}. \tag{6b}$$

To lowest order in τ, (5) yields

$$\tau_n \simeq \frac{2\alpha(\mu_n - \beta\sin\phi_n)}{1 + \alpha\beta\cos\phi_n}. \tag{7}$$

With the substitution of (7) into (6a), the set (6) gives the first order change in velocity and the zero order change in phase which transforms the velocity and phase just before the n^{th} entry into the sheath to that just before the $(n+1)^{st}$ entry:

$$\mu_{n+1} = -\mu_n + \frac{2(\mu_n - \beta\sin\phi_n)}{1 + \alpha\beta\cos\phi_n}, \tag{8a}$$

$$\phi_{n+1} = \phi_n + \frac{1}{\epsilon\mu_{n+1}}. \tag{8b}$$

To insure measure preservation for the Hamiltonian mapping (8), the change in phase must also be determined to first order. Furthermore, the variables μ and ϕ are not canonically conjugate in a Hamiltonian sense [11]. For the surface of section at a constant position, the electron energy E and the crossing time t are canonically conjugate; the equivalent normalized variables are $\mathcal{E} = \mu^2$ and $\phi = \omega t$. The Hamiltonian mapping is area preserving in these canonically conjugate variables. Assuming a small energy change, $\mathcal{E}_{n+1} - \mathcal{E}_n \ll \mathcal{E}_n$,

expanding (8a) for small α, and determining the first order change in phase in the usual manner [11] to insure area preservation, (8) becomes

$$\mathcal{E}_{n+1} = \mathcal{E}_n - 4\beta\sqrt{\mathcal{E}_{n+1}}\sin\phi_n + 4\alpha\beta\mathcal{E}_{n+1}\cos\phi_n, \tag{9a}$$

$$\phi_{n+1} = \phi_n + \frac{1}{\epsilon\sqrt{\mathcal{E}_{n+1}}} + \frac{2\beta\cos\phi_n}{\sqrt{\mathcal{E}_{n+1}}} + 4\alpha\beta\sin\phi_n. \tag{9b}$$

Over most of the phase space the last term on the right of (9a) is small and can be dropped, along with its area preserving counterpart, the last term in (9b). In this approximation the change in velocity in one pass through the sheath is just

$$\Delta v = v_{n+1} - v_n = -2\omega s_0 \frac{V_{rf}}{V_{dc}}\sin\phi_n, \tag{10}$$

which is the impulse approximation of the Fermi acceleration mapping [8]. This approximation has also been used by Godyak and associates [1–5], together with the assumption that ϕ_n is a random variable, to treat the sheath heating without employing mapping theory.

From the map (9) the main features of the dynamics can be deduced. The change in energy is proportional to ω, with the energy dependence $\Delta\mathcal{E} \propto \sqrt{\mathcal{E}}$. Electrons moving according to these dynamics will experience regular or chaotic motion in different regions of the parameter space. It is possible to estimate the particle energies for which transitions from regular to stochastic motion will occur. Through the appropriate change of variables, this map can be put in the form of the Chirikov standard map [11,14]

$$I_{n+1} = I_n + K\sin\theta_n,$$

$$\theta_{n+1} = \theta_n + I_{n+1}.$$

As is well known, chaotic motion occurs in this map for $K > 1$. Thus knowing the value of K gives a measure of the stochasticity in the system.

To get a local approximation of the stochasticity parameter for the mapping (9), expand about a fixed point $(\bar{\mathcal{E}}_k, \bar{\phi}_k)$ of (9), $\mathcal{E}_n = \bar{\mathcal{E}}_k + \Delta\mathcal{E}_n$ and $\phi_n = \bar{\phi}_k + \Delta\phi_n$, to obtain

$$\Delta\mathcal{E}_{n+1} = \Delta\mathcal{E}_n + 4\beta\sqrt{\bar{\mathcal{E}}_k}\sin\Delta\phi_n,$$
$$\Delta\phi_{n+1} = \Delta\phi_n - \left[\frac{1}{2\epsilon\bar{\mathcal{E}}_k^{3/2}} + \frac{\beta}{\bar{\mathcal{E}}_k^{3/2}}\right]\Delta\mathcal{E}_{n+1}.$$

With the substitution

$$I_{n+1} = -\frac{1+2\epsilon\beta}{2\epsilon\bar{\mathcal{E}}_k^{3/2}}\Delta\mathcal{E}_{n+1},$$

this takes the form of the standard map. Thus, using $\epsilon \ll 1$, the approximate stochasticity parameter describing (9) is, in terms of the dimensional electron energy, E,

$$K = \frac{\alpha\beta e V_{dc}}{\epsilon E}.$$

As can be seen, K decreases with increasing energy, so the system is less stochastic at higher energies. This occurs because as the energy increases, the phase shift across the plasma decreases, and phase correlations between successive collisions with the sheaths reduce the stochasticity. The condition for stochastic motion in physical variables is

$$E < m_e\omega^2 s_0 l\frac{V_{rf}}{V_{dc}}. \tag{11}$$

Using some values for a high frequency r.f. discharge: $l = 10$ cm, $s_0 = 0.025$ cm, $V_{rf} = 100$ volts, $V_{dc} = 110$ volts and $\omega/2\pi = 100$ MHz, the condition for stochasticity is $E \lesssim 50$ eV.

The easiest way to visualize the dynamics is to plot a surface of section of the phase space. By plotting the electron energy versus the phase of the r.f. field each time an electron leaves the sheath, a picture of the dynamics is developed. Figure 1 shows this surface of section for the dynamics given by (9). The parameters of the map are representative of

r.f. discharges. The low energy portion of the phase space is entirely stochastic, and the stochasticity decreases with increasing energy, as predicted by (11). This results in a barrier to heating, which for the parameters chosen occurs at $E \sim 150$ eV. In a physical discharge, electrons will escape through the sheath when they reach an energy

$$E > V_{dc}(1 - \beta \cos \phi). \tag{12}$$

Since electrons must always be able to escape in a physical system, at some phases this energy must lie below the heating barrier, and the phase space will be chaotic; a typical escape energy is shown as the solid curve. Thus electrons will be heated by the stochastic dynamics until they reach the escape curve; in numerical simulations of the discharge, such electrons are removed from the simulation and replaced by low energy electrons, modeling the ionization process.

While these sections are useful to illustrate the mapping dynamics, they are not the most useful description of the physical system. Since fast electrons interact more frequently with the sheaths than slow electrons during a given time interval, maps taken at a constant surface in space cannot be used directly to predict physical quantities. By iterating each electron for an equal time instead of between successive sheath interactions, an alternative surface of section can be developed. The proper canonical variables for this surface are the electron velocity and the physical position of the electron in the plasma; this is shown in Figure 2 for the same parameters as in Figure 1, but instead of looking at the system after each collision with the sheath, a "snapshot" of the electrons is taken at equal time intervals. If these intervals are multiples of the r.f. period then this procedure gives a proper surface of

section, and the corresponding maps can be used to make physically significant predictions, such as the energy dependence of the electron distribution.

3. Fokker-Planck Calculation

Electrons moving under stochastic dynamics will diffuse in energy and phase throughout the available phase space. In the general case, if we have a two dimensional equal time mapping in velocity v and position x, and we are in a stochastic region of phase space, then by making the random phase approximation we can describe the system in terms of a distribution function in v alone. The evolution of this distribution function $f(v,t)$ is given by [11]

$$\frac{\partial f(v,t)}{\partial t} = -\frac{\partial}{\partial v}(B(v)f(v,t)) + \frac{\partial}{\partial v}\left[\frac{D(v)}{2}\frac{\partial}{\partial v}f(v,t)\right]. \tag{13}$$

Since time is the physically relevant independent variable for the distribution function, the local diffusion coefficient $D(v)$ and frictional coefficient $B(v)$ are determined from the equal time mapping. Once $f(v,t)$ is known, we can calculate quantities such as the average electron energy and the rate of ionization.

Since we are interested in the regime where the stochastic heating dominates, collisions lead to phase randomization and isotropization but not dissipation, and we calculate the distribution function from (13) with $B(v) = 0$. The quasi-linear diffusion coefficient is given by

$$D(v) = \frac{\int dx(\Delta v_T(v,x))^2}{\int dx},$$

where Δv_T is the Hamiltonian velocity change for the period T, and the integral is over all x possible for the mapping period T.

To calculate $D(v)$ analytically, we use the constant position map and make the appropriate transformation. If we assume a time step of length T, and neglect the time spent in the sheath compared to the transit time across the body of the plasma, then the number of bounces in time T for an electron with velocity v is just $N = Tv/l$. Then if we know the velocity change $\Delta v(v, x)$ for one bounce, the diffusion coefficient will be

$$D(v) = \frac{N}{T} \frac{\int dx (\Delta v(v,x))^2}{\int dx},$$

where the integral is over all x and $\Delta v(v, x)$ is the velocity change for a single bounce. Using $x = v\phi/\omega$ and writing $D(v)$ in terms of μ, the normalized velocity, gives

$$D(\mu) = \frac{N}{2\pi T} \int_0^{2\pi} d\phi (\Delta\mu(\mu, \phi))^2.$$

These transformations allow the use of the constant position map (9) to calculate $D(\mu)$.

To lowest order, the one dimensional normalized velocity change is

$$\Delta\mu(\mu, \phi) = -2\beta \sin\phi.$$

Thus, we obtain

$$D(\mu) = 2\epsilon\beta^2\mu. \tag{14}$$

Since we are looking for a steady-state solution, we set $\partial f/\partial t = 0$ and integrate over μ. In the physical system, there will be a particle flux; electrons are born at low energy through

ionization and escape through the sheath at high energy. Thus, in the steady state, (13) becomes

$$\Gamma = -\frac{D(\mu)}{2}\frac{\partial}{\partial \mu} f(\mu) = \text{constant}, \tag{15}$$

where Γ is the electron flux through the system. This can be integrated and $f(\mu)$ can be found by applying the appropriate boundary conditions. The boundary at $\mu = 0$ is perfectly reflecting, so the boundary conditions there are $f(\mu) \neq 0$ and $\Gamma = 0$. We postulate a source at $\mu = \mu_0$ to model the creation of electrons through ionization, so $\Gamma = 0$ for $\mu < \mu_0$ and $\Gamma \neq 0$ for $\mu > \mu_0$. If we model the escape surface in phase space as a constant velocity $\mu = \mu_m$, then the boundary conditions at $\mu = \mu_m$ are $f(\mu_m) = 0$ and $\Gamma \neq 0$. Substituting (14) into (15), we obtain

$$f(\mu) \propto \ln \frac{\mu_m}{\mu}$$

in the region $\mu_0 < \mu < \mu_m$. In the region $0 < \mu < \mu_0$, $f(\mu) = \text{constant}$. In terms of energy $\mathcal{E} = \mu^2$, we have the scaling $f(\mu)d\mu = f(\mathcal{E})d\mathcal{E}$, such that for $\mu_0 < \mu < \mu_m$,

$$f(\mathcal{E}) \propto \frac{\ln(\mathcal{E}_m/\mathcal{E})}{\sqrt{\mathcal{E}}}. \tag{16}$$

Figure 3 compares the distribution function obtained by iterating the exact area preserving map to the analytic distribution of the same average energy. The solid line is the numerical distribution, and the dashed line is the distribution predicted by (16). Both distributions are normalized so that $\int f(E)dE = 1$. To determine the numerical distribution, an ensemble of 4000 electrons was started with energies between 0.05 and 0.15 eV and was allowed to accelerate under the chaotic dynamics. Electrons were removed from the distribution according to (12) and new electrons were injected at low energy (between 0.05 and 0.15 eV).

The agreement is quite good over the energy range between the injection energy and the energy at which electrons are lost. The numerical distribution falls off more slowly at high energy because electrons escape over a range of energies, not at a single $E = E_m$. At low energies the bump in the distribution reflects the electron source at 0.1 eV.

The calculation of the electron distribution must be modified for a three dimensional system. Since only the parallel velocity is affected by the sheath interaction, we have, in terms of the normalized velocity $\boldsymbol{\mu} = (\mu_x, \mu_y, \mu_z)$,

$$|\boldsymbol{\mu}|^2_{n+1} = (\mu_x)^2_n + (\mu_y)^2_n + (\mu_z + \Delta\mu_z)^2_n,$$

where $\Delta\mu_z = -2\beta \sin\phi$.

By the ordering (1), collisions with neutrals act to scatter the electrons on a time scale which is long compared to the typical bounce time but short compared to the electron lifetime, resulting in an isotropic distribution. To model the scattering we write the mapping as a function of the magnitude of the velocity, $|\boldsymbol{\mu}|$, only:

$$|\boldsymbol{\mu}|_{n+1} = |\boldsymbol{\mu}|_n + \Delta|\boldsymbol{\mu}|,$$

where

$$\Delta|\boldsymbol{\mu}| = \sqrt{|\boldsymbol{\mu}|^2 + 2\mu_z\Delta\mu_z + (\Delta\mu_z)^2} - |\boldsymbol{\mu}|.$$

By writing $\mu_z = |\boldsymbol{\mu}| \cos\xi$ and integrating over angles, we obtain

$$\Delta|\boldsymbol{\mu}| = \frac{\Delta\mu_z}{2},$$

and the three dimensional diffusion coefficient is then

$$D(|\boldsymbol{\mu}|) = \frac{\epsilon\beta^2|\boldsymbol{\mu}|}{2}. \tag{17}$$

The three dimensional distribution function $g(\mu)$ satisfies the equation

$$\nabla_\mu \left(\frac{D(|\mu|)}{2} \nabla_\mu g(\mu) \right) = 0.$$

Since the electron distribution is isotropic and the diffusion coefficient is independent of angle, the distribution function will be a function of $|\mu|$ only, so in the steady state

$$|\mu|^2 \Gamma = -|\mu|^2 \frac{D(|\mu|)}{2} \frac{\partial}{\partial |\mu|} g(|\mu|) = \text{constant},$$

which leads to the distribution

$$g(|\mu|) \propto \frac{1}{|\mu|^2} - \frac{1}{|\mu_m|^2},$$

where, as before, $|\mu_m|$ is the escape velocity of the electrons. In three dimensions we have the scaling $g(\mu) d^3\mu = g(\mathcal{E}) d\mathcal{E}$, so

$$g(\mathcal{E}) \propto \sqrt{\mathcal{E}} \left(\frac{1}{\mathcal{E}} - \frac{1}{\mathcal{E}_m} \right). \tag{18}$$

Figure 4 compares this distribution with a three dimensional Maxwellian distribution of the same average energy. The normalization for both is $\int g(v) d^3v = 1$. The distribution given by equation (18) contains more electrons at both high and low energies than the Maxwellian; this behavior is representative of this distribution, and is independent of the average energy of the distributions. Godyak and Oks [13] have measured a qualitatively similar distribution for high frequency, low pressure r.f. discharges.

4. Self-Consistent Model

Thus far the dynamics of a single particle has been examined using a set of arbitrary

parameters. By adding physical constraints to the single particle dynamics we obtain a self-consistent model of the discharge. It is assumed that V_{rf}, ω, $p_0 l$ and M, the ion mass, are the control parameters, and the model will be used to determine V_{dc}, T_e, s_0 and n_e.

One self-consistency condition is that the rate of ionization must equal the rate of ion loss out of the plasma; that is,

$$\langle \nu^z \rangle \frac{l}{2} = 0.606 u_B, \tag{19}$$

where

$$\langle \nu^z \rangle = \frac{n_0}{\sqrt{m_e}} \int g(E) \sigma^z(E) \sqrt{E} dE,$$

$$\sigma^z(E) = \frac{4\sigma_0^z E_z}{E} \left[1 - \frac{E_z}{E} \right],$$

$$\sigma_0^z \simeq 3 \times 10^{-16} \text{ cm}^2, \qquad E_z = 15.76 \text{ eV},$$

and the ions are assumed to enter the sheath with a density 0.606 times the central density and with the Bohm velocity $u_B = \sqrt{T_e/M}$. Thus (19) relates the electron temperature T_e to $p_0 l$, where $T_e = (2/3)\langle E_e \rangle$ for a three dimensional distribution, $T_e = 2\langle E_e \rangle$ for a one dimensional distribution, and $\langle E_e \rangle$ is the average electron energy.

A second self-consistency condition is the relationship between the r.f. and d.c. electric fields in the sheath, that is, the connection between V_{rf} and V_{dc}. Equating the electron and ion loss rates, we have, approximately [15]

$$V_{dc} = V_{rf} + CT_e, \tag{20}$$

where $C \simeq \ln \sqrt{M/m_e}$. This gives an estimate of V_{dc} which can be used in the analytic model. However, in order to calculate those quantities which depend on the electron escape energy, such as the electron flux, it is necessary to know the difference between V_{dc} and V_{rf}

more precisely. In the next section a procedure to obtain a more precise estimate from a numerical simulation of the discharge is given.

A third self-consistency condition is the Child-Langmuir law for ions

$$\Gamma_i = 0.606 n_e u_B = \frac{4}{9}\left(\frac{2e}{M}\right)^{1/2} \frac{\epsilon_0 |V_{dc}|^{3/2}}{e s_0^2}, \tag{21}$$

which relates s_0 to T_e and n_e.

The final condition required to obtain a complete self-consistent set of equations is the electron energy balance in the plasma. To calculate the power injected into the plasma electrons through stochastic heating, we first consider the energy transferred to a single electron by one collision with the sheath, $\Delta E \equiv E_f - E_i$. In general, ΔE is a function of both the electron velocity, v, and the position of the sheath boundary when the electron enters the sheath, through the phase variable ϕ. ΔE can be calculated from the velocity change in the sheath given by equation (10)

$$\Delta E(v,\phi) = \frac{m_e}{2}(v_f^2 - v^2) = \frac{m_e}{2}\Delta v(v,\phi)(\Delta v(v,\phi) + 2v),$$

where $\Delta v(v,\phi) = v_f - v$.

If T, the period of the equal time map, is large compared to l/v, the transit time across the plasma, then an electron makes Tv/l bounces during each iteration of the map. To calculate the average energy change, assume that the electron phase θ is uniformly distributed and average over it. Since the sheath boundary is moving, however, the flux of electrons hitting the sheath is a function of time, and ϕ is not uniformly distributed. If θ is the random phase variable, then ϕ is distributed according to

$$d\theta = (1 - \frac{\omega s_0 \beta}{v}\sin\phi)d\phi.$$

Thus the average power injected into an electron at a given velocity is

$$P(v) = \frac{Tv}{l}\frac{1}{2\pi T}\int d\theta \Delta E(v,\phi),$$

where $(2\pi)^{-1}\int d\theta \Delta E$ is the phase average of the energy transfer per collision. The total power into the plasma is then

$$P = \int P(v) g(\boldsymbol{v}) d^3v.$$

Integrating over the distribution (18) yields

$$P = 2m_e\omega^2 s_0^2 \beta^2 \Gamma_s, \tag{22}$$

where Γ_s is the electron flux hitting the sheath.

The power into the electrons must be equal to the power carried from the plasma when electrons escape across the sheaths plus the power the electrons lose to collisions with neutrals. Thus,

$$P = \Gamma E_m + n_e \nu^z l e U_L, \tag{23}$$

where Γ is the electron flux out of the plasma, $E_m \propto V_{dc} - V_{rf}$ is the typical energy of an escaping electron as it enters the sheath, and the second term represents the power lost by the electrons due to excitation and ionization. Equations (22) and (23) also relate the electron density n_e to s_0 and T_e.

The equations (19)–(23) form a self-consistent model of an r.f. discharge. Given the control parameters V_{rf}, ω, $p_0 l$ and M, and the underlying dynamics of the discharge, this set of equations determines the state of the discharge as characterized by V_{dc}, T_e, s_0 and n_e. These results are shown in Figure 5 for an argon discharge operating at $V_{rf} = 100$ volts and

$\omega/2\pi = 100$ MHz. Figure 5a shows the average electron energy as a function of $p_0 l$ for this discharge, while Figure 5b shows the corresponding electron density.

We check that these results over this pressure range are consistent with condition (1) on the various timescales of interest. For a discharge of length l, the mean bounce time for an electron with parallel velocity $v_{||}$ is given by

$$\tau_b = \int d^3v g(v) \frac{l}{v_{||}}.$$

Since the electron lifetime must equal the ion lifetime, by assuming a Bohm velocity for the ions at the sheath edge τ_l can be simply estimated as

$$\tau_l = \frac{l}{2}\sqrt{\frac{M}{T_e}}.$$

The collision times are the inverse of the collision frequencies

$$\langle \nu \rangle = n_0 \int d^3v g(v) v \sigma(v),$$

where the appropriate cross-section for elastic or inelastic scattering (σ^c or σ^z) is used. For a typical argon discharge the time ordering (1) holds in the pressure range $1.0 < p_0 l <$ 10.0 mTorr-cm, as shown in Figure 6. In the pressure range $p_0 l < 1.0$ mTorr-cm, the electron lifetime is less than the mean time for elastic collisions, and the distribution is not isotropized by elastic collisions. In this regime, the system is more properly treated as a one dimensional system, with elastic scattering into the other dimensions modeled as a frictional drag. In the pressure range $p_0 l > 10.0$ mTorr-cm, elastic collisions act to phase randomize the electrons every bounce, and the single particle dynamics must be modified accordingly. In both cases, however, stochastic heating still occurs, and we expect the results to be qualitatively the same.

5. Many Particle Simulation

As a check on the self-consistent model given by (19)–(23) we compare a one dimensional self-consistent model with a one dimensional numerical simulation of the discharge. The one dimensional model is described by equations (19)–(23), with the substitution of the one dimensional electron distribution (16) for the three dimensional distribution (18). To simulate the discharge, we begin with an ensemble of low energy ($\sim$ 0.1 eV) electrons and allow them to evolve under the dynamics. As the simulation proceeds, the electrons are stochastically heated by the oscillating sheath fields. Electrons reaching a sufficiently high energy pass completely through the sheath and recombine at the wall. In the simulation this is done explicitly by following the electron orbits in the sheath and removing from the simulation those electrons which transverse the entire sheath. As electrons are removed from the simulation they are replaced by low energy electrons, modelling the creation of free electrons through ionization. Eventually the electron distribution reaches a steady state, with electrons diffusing from low to high energy.

Since this steady state depends on the electron escape curve [as shown in (12)], and the escape curve is a function of the difference $V_{dc} - V_{rf}$, V_{dc} must be determined dynamically by the simulation. This is done by allowing V_{dc} to vary in time as the simulation proceeds. Since the average electron lifetime is controlled by the stochastic heating (as the heating increases [decreases], the average lifetime decreases [increases]), the parameter β (the ratio V_{rf}/V_{dc}) controls the electron lifetime through the rate of stochastic heating. We therefore tie the d.c. potential to the mean electron energy through the relation

$$V_{dc} = V_{rf} + C\langle E_e \rangle.$$

The motivation for this equation is as follows: if $V_{rf} = 0$, corresponding to $\beta = 0$, then the confining potential required to make electron and ion losses equal is just some constant C times the average electron energy. In the presence of the r.f. field, the d.c. field is larger than the amplitude of the r.f. field by a similar factor. As the simulation progresses, a steady state will result: if the average energy rises, V_{dc} will increase, resulting in a lower heating rate; if the average electron energy drops, V_{dc} will decrease and the heating will increase. The parameter C controls the relationship between the stochastic heating rate and the height of the electron escape curve.

Additionally, the electron lifetime (as determined by the simulation) determines the ion mass. From quasi-neutrality of the plasma the average lifetime of the ions and electrons must be the same: $\langle t_i \rangle = \langle t_e \rangle \equiv \langle t \rangle$. By setting the average ion velocity to be $v = l/2\langle t \rangle$, and assuming a Bohm energy, $E_i = T_e/2$, for the ions as they enter the sheath, the ion mass as a function of the average electron lifetime and energy can be calculated:

$$M_i = \frac{4T_e\langle t \rangle^2}{l^2}.$$

Thus by adjusting C in the simulation, the height of the electron escape curve can be moved so that a plasma of any desired ion mass can be simulated.

The simulation of the plasma uses V_{rf}, ω, l, s_0 and C as input parameters. Exploring the C–s_0 plane corresponds to simulating discharges of differing ion mass and pressure. For a given choice of C and s_0, we begin with an ensemble of low energy electrons and allow them to evolve under the dynamics. As the simulation progresses, a steady state is reached. From the average electron lifetime the corresponding ion mass can be calculated. The simulation also determines the electron distribution and average energy. Using the analytic distribution

(16) with the same average energy, we calculate the self-consistent pressure from (19). By varying C and s_0 so that the ion mass remains constant, the average energy is found as a function of $p_0 l$. This curve is shown in Figure 7a for an argon discharge operating at $V_{rf} = 100$ volts and $\omega/2\pi = 100$ MHz. Since the mass is not held exactly constant during this iterative procedure, the numerical points (shown as crosses) differ slightly from the solution in which the mass is held constant at $M = 40M_p$ (shown as the dotted line).

In Figure 7b, the numerically determined density is compared to the analytic density obtained using (21)–(23). Using the values of V_{dc} and $\langle E_e \rangle$ obtained from the simulation, along with the value of s_0 input into the simulation, the numerical value ofn_e is calculated from (21). This is shown as the crosses in Figure 7b. The dotted line shows the value of n_e obtained from a completely analytic solution of (19)–(23) in the one dimensional case. The primary reasons for the differences between the numerical density and the analytic density are (a) in the exact dynamics of the simulation, electrons can escape through the sheath over a range of energy, not at a single energy as used in the analytic model; (b) the constant C varies in the simulation; in Figure 7, C varies between 3.9 and 4.3, while in the analytic model it is held constant at $C = \ln\sqrt{M/m_e} \simeq 5.6$; (c) the electron distribution (16) predicted by quasi-linear theory differs slightly from the actual numerical distribution. However, the good agreement between the numerics and theory verifies the approximations used in deriving (19)–(23).

6. Discussion and Conclusions

We have explored a mechanism of plasma heating in an r.f. discharge, that of energy transfer on reflection from the oscillating sheaths. This mechanism may dominate over bulk plasma heating over some range of r.f. and plasma parameters. Specifically, there is an onset of collisionless plasma heating as the r.f. frequency is raised above a threshold level which is typically well above the usual range of r.f. discharge frequencies. For a typical configuration considered here, this threshold occurs at $\omega/2\pi > 50$ MHz and in a pressure range $p_0 l \leq 10$ mTorr-cm. The analysis of this paper only holds in this pressure range, as only isotropization associated with electron-neutral elastic scattering collisional processes have been treated.

Although the collisionless heating may be strong compared to collisional heating processes, the resulting average electron temperature is similar to that occurring at lower frequencies with collisional heating. This result is a consequence of the fact that the electron temperature is determined by a competition between ion losses, set primarily by the electron temperature, and ionization, set also by the electron temperature, and thus is independent of the heating strength. The key difference between the sheath heating mechanism, described here, and the more usual collisional heating mechanism is the power law distribution of energy $f(E) \propto E^{-1/2}$, rather than the usual Maxwellian distribution $f(E) \propto e^{-E/kT}$, resulting in both more slow and more fast moving electrons, as shown in Figure 4, and an increased ionization efficiency, compared to a Maxwellian.

In the preceding analysis no attempt has been made to optimize parameters for any specific purpose. We have chosen rather to demonstrate the generic features of an r.f. dis-

charge that is heated by collisionless interaction with the sheath, and have shown that the discharge parameters can be chosen self-consistently, Thus we can expect that a laboratory plasma can be created having the basic distributions described in this paper.

We do not, however, consider these results to be a complete study of a high frequency r.f. plasma discharge. In particular, the simplified sheath model presented here is only an approximation to the highly nonlinear sheath dynamics. From studies of d.c. discharges [12] it is evident that the sheath conditions used here are overly idealized. More generally, a self-consistent solution of the dynamics, including the nonlinear oscillation of the sheath boundary should be employed [16]. Additionally, non-uniformity of the bulk plasma, collisional breaking of the invariants at high pressure and low frequency, and the transition to parameter ranges in which the sheath and bulk heating compete should be considered. Ultimately, experimental measurement of the distribution function of the electrons would be a key test of the theoretical predictions.

The preceeding results are also of non-trivial interest for the theory of area preserving mappings. They indicate that self-consistent numerical solutions to mapping problems can be generated in which the external parameters driving the dynamics are continuously adjusted to satisfy the self-consistency conditions. The procedure is stable and converges to a self-consistent solution. Thus, while we have used the power of mapping theory to gain insight into the processes of collisionless heating in an r.f. discharge, we have also shown how mapping theory can be extended to include self-consistent conditions.

The support for this work provided by National Science Foundation Grant ECS-8517363 and Department of Energy Grant DE-FG03-87ER13727 is gratefully acknowledged.

Figure Captions

Figure 1. Constant position phase portrait ($\alpha = 0.0073$, $\beta = 0.833$, $\epsilon = 0.005$). Solid line shows energy above which electrons transverse the entire sheath and recombine with the wall.

Figure 2. Equal time phase portrait for same parameters as Figure 1.

Figure 3. Comparison of numerical and analytic one dimensional electron distributions of the same average energy. Both distributions are normalized to one.

Figure 4. Comparison of analytic three dimensional electron distribution with a Maxwellian of the same average energy. Both distributions are normalized to one.

Figure 5. Pressure dependence of a three dimensional r.f. discharge. a) Average electron energy *vs* pressure ($V = 100$ Volts, $\omega/2\pi = 100$ MHz, $M = 40M_p$. b) Electron density *vs* pressure.

Figure 6. Time ordering for a typical argon discharge.

Figure 7. Pressure dependence of a one dimensional r.f. discharge. a) Average electron energy *vs* pressure ($V = 100$ Volts, $\omega/2\pi = 100$ MHz, $M = 40M_p$. b) Electron density *vs* pressure. [+ Numerical, $\cdots$ Theoretical]

References

[1] V. A. Godyak, Sov. Phys. Tech. 16 1073 (1972).

[2] V. A. Godyak, Sov. J. Plasma Phys. 2 78 (1976).

[3] V. A. Godyak and Z. Kh. Ganna, Sov. J. Plasma Phys. 5 376 (1979).

[4] V. A. Godyak and Z. Kh. Ganna, Sov. J. Plasma Phys. 6 372 (1980).

[5] O. A. Popov and V. A. Godyak, J. Appl. Phys. 57 53 (1985).

[6] A. I. Akiezer and A. S. Bakai, Sov. Phys. Dokl. 16 1065 (1971).

[7] A. I. Akiezer and A. S. Bakai, Sov. J. Plasma Phys. 2 359 (1976).

[8] E. Fermi, Phys. Rev. 75 1169.

[9] G. M. Zaslavski and B. V. Chirikov, Sov. Phys. Dokl. 9 989 (1969).

[10] M. A. Lieberman and A. J. Lichtenberg, Phys. Rev. A5 1852 (1972).

[11] A. J. Lichtenberg and M. A. Lieberman, Regular and Stochastic Motion Springer-Verlag N. Y. 1983.

[12] G. A. Emmert, Phys. Fluids 23 203 (1980).

[13] V. A. Godyak and S. N. Oks, Sov. Phys. Tech. 24 1255 (1979).

[14] B. V. Chirikov, Phys. Reports 52 265 (1979).

[15] J. H. Keller and W. B. Pennebaker, IBM J. Res. Develop. 23 3 (1979).

[16] M. A. Lieberman, to appear in the IEEE Transactions on Plasma Science (1988).

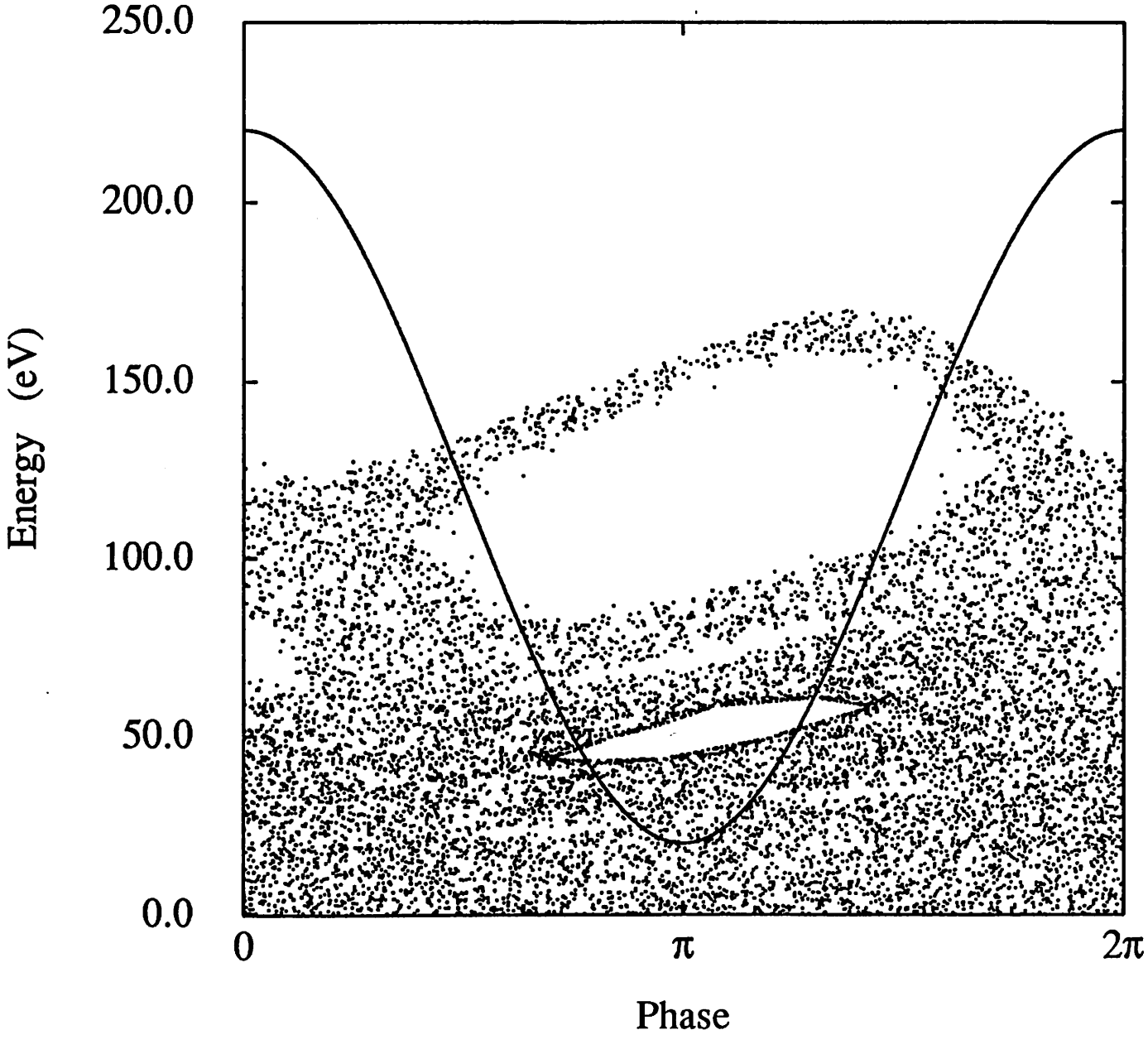
250.0
200.0
150.0
100.0
50.0
0.0
Energy (eV)
0
π
2π
Phase

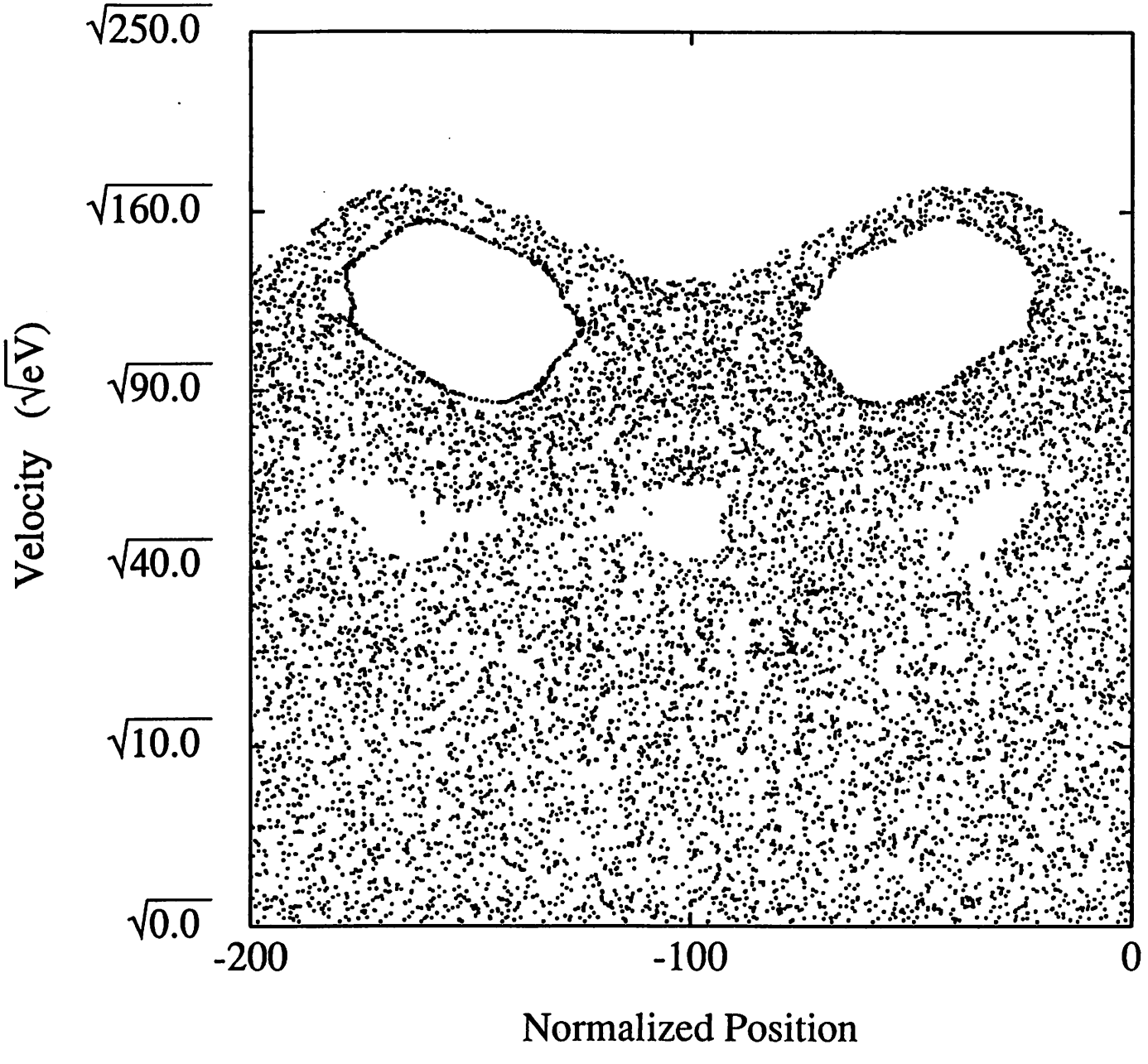
√250.0
√160.0
√90.0
√40.0
√10.0
√0.0
Velocity (√eV)
-200
-100
0
Normalized Position

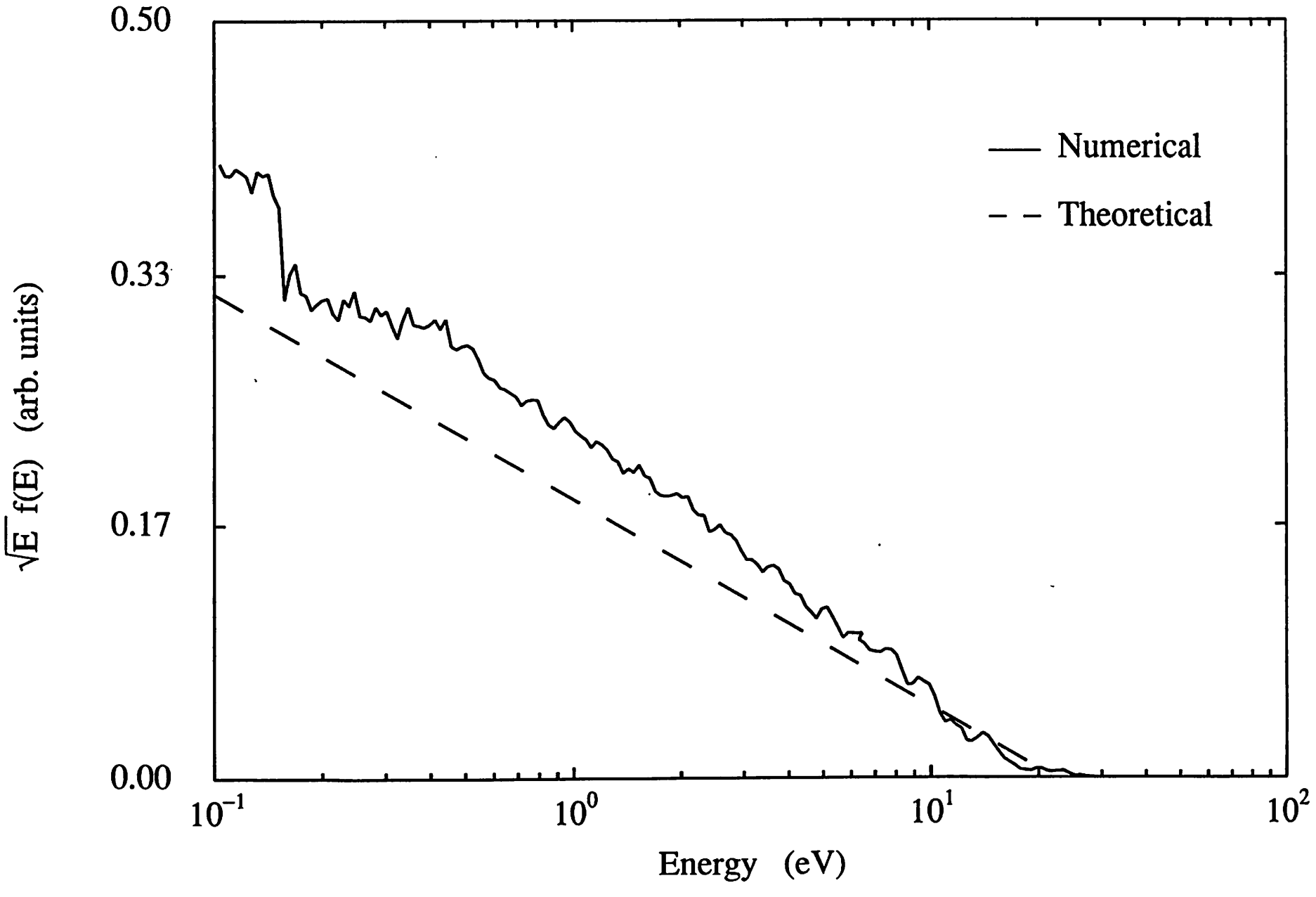
0.50
0.33
0.17
0.00
$\sqrt{E}$ f(E) (arb. units)
10^{-1}
10^{0}
10^{1}
10^{2}
Energy (eV)
Numerical
Theoretical

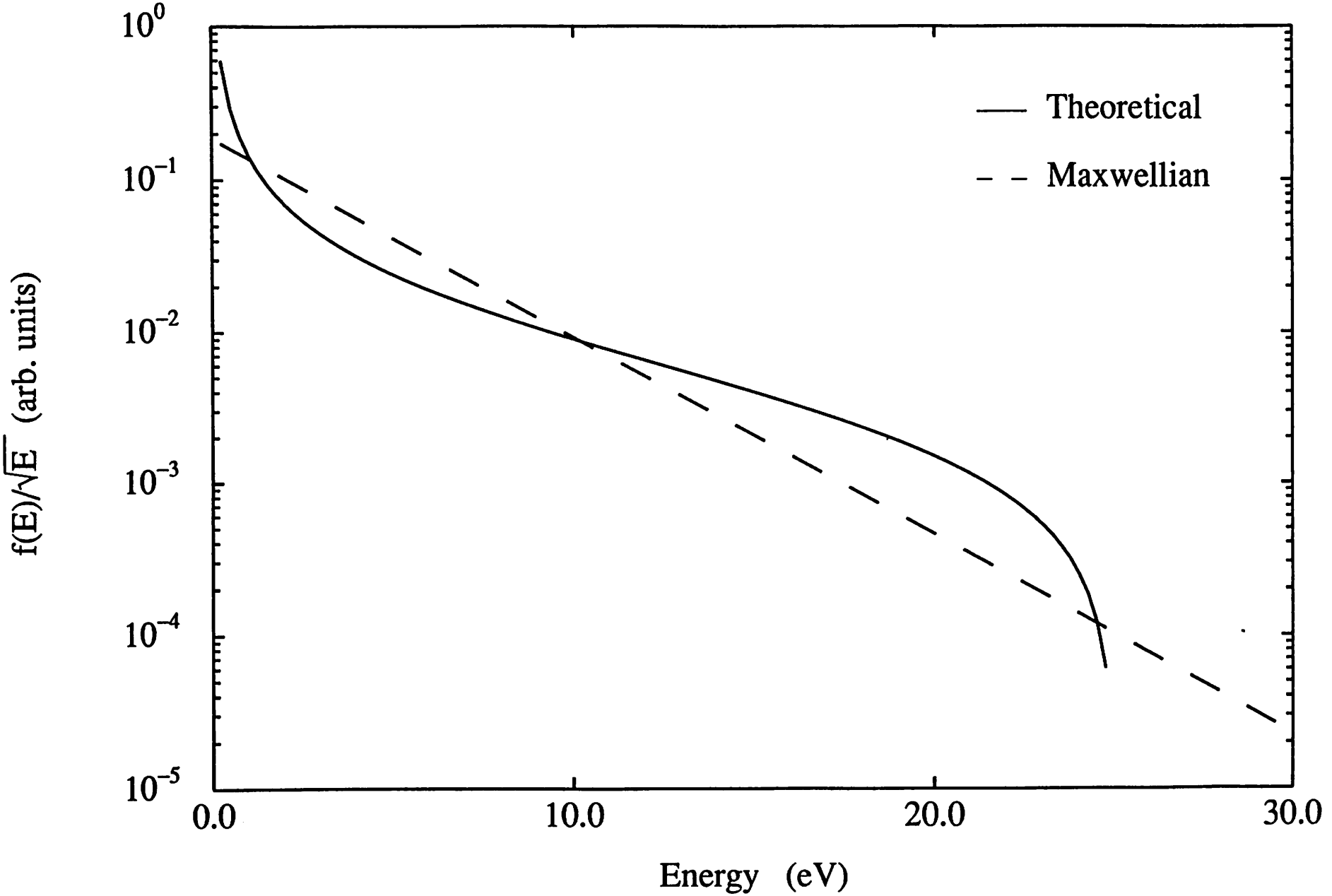
10^0
10^{-1}
10^{-2}
10^{-3}
10^{-4}
10^{-5}
$f(E)/\sqrt{E}$ (arb. units)
0.0
10.0
20.0
30.0
Energy (eV)
Theoretical
Maxwellian

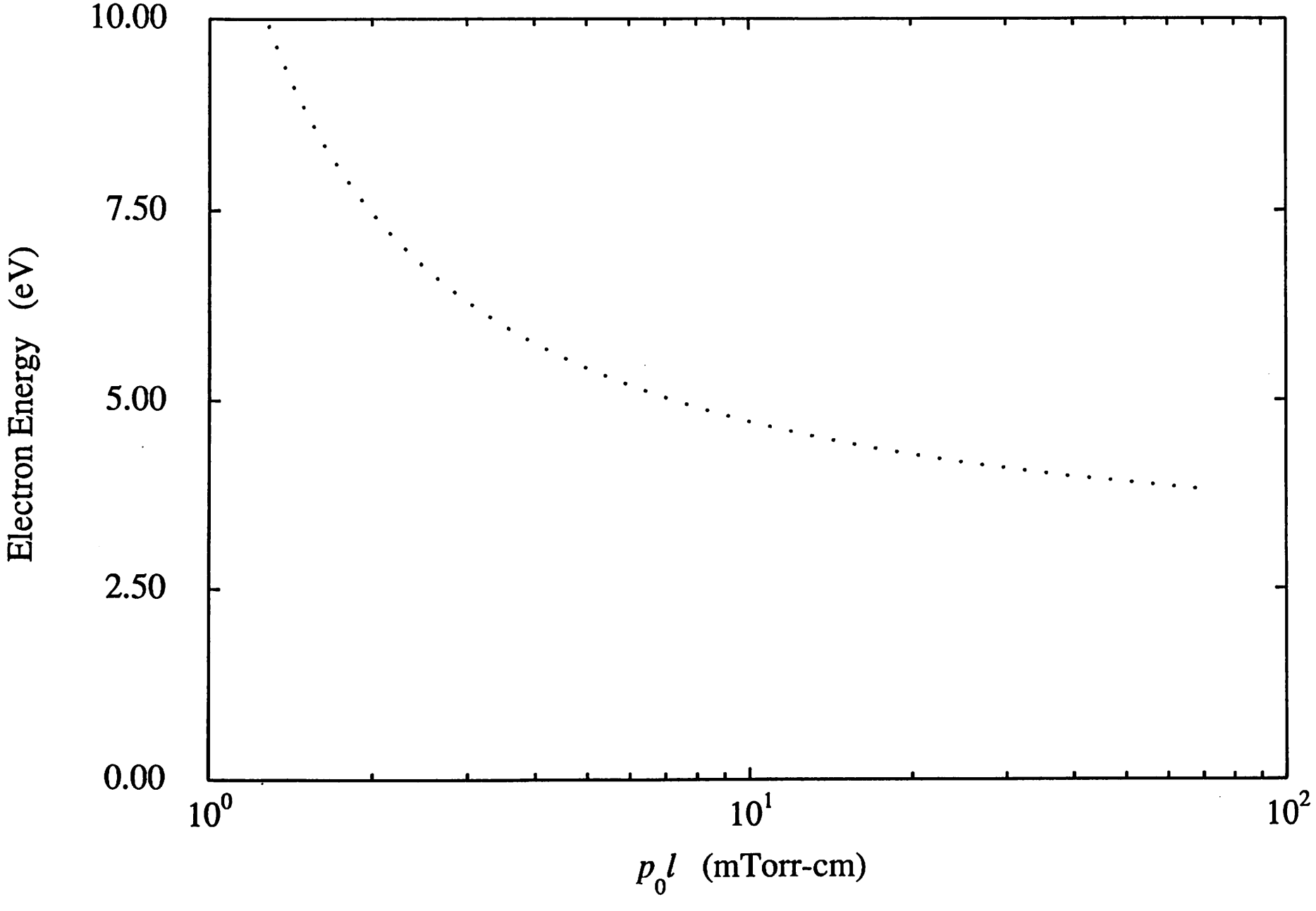
10.00
7.50
5.00
2.50
0.00
Electron Energy (eV)
10^0
10^1
10^2
$p_0 l$ (mTorr-cm)

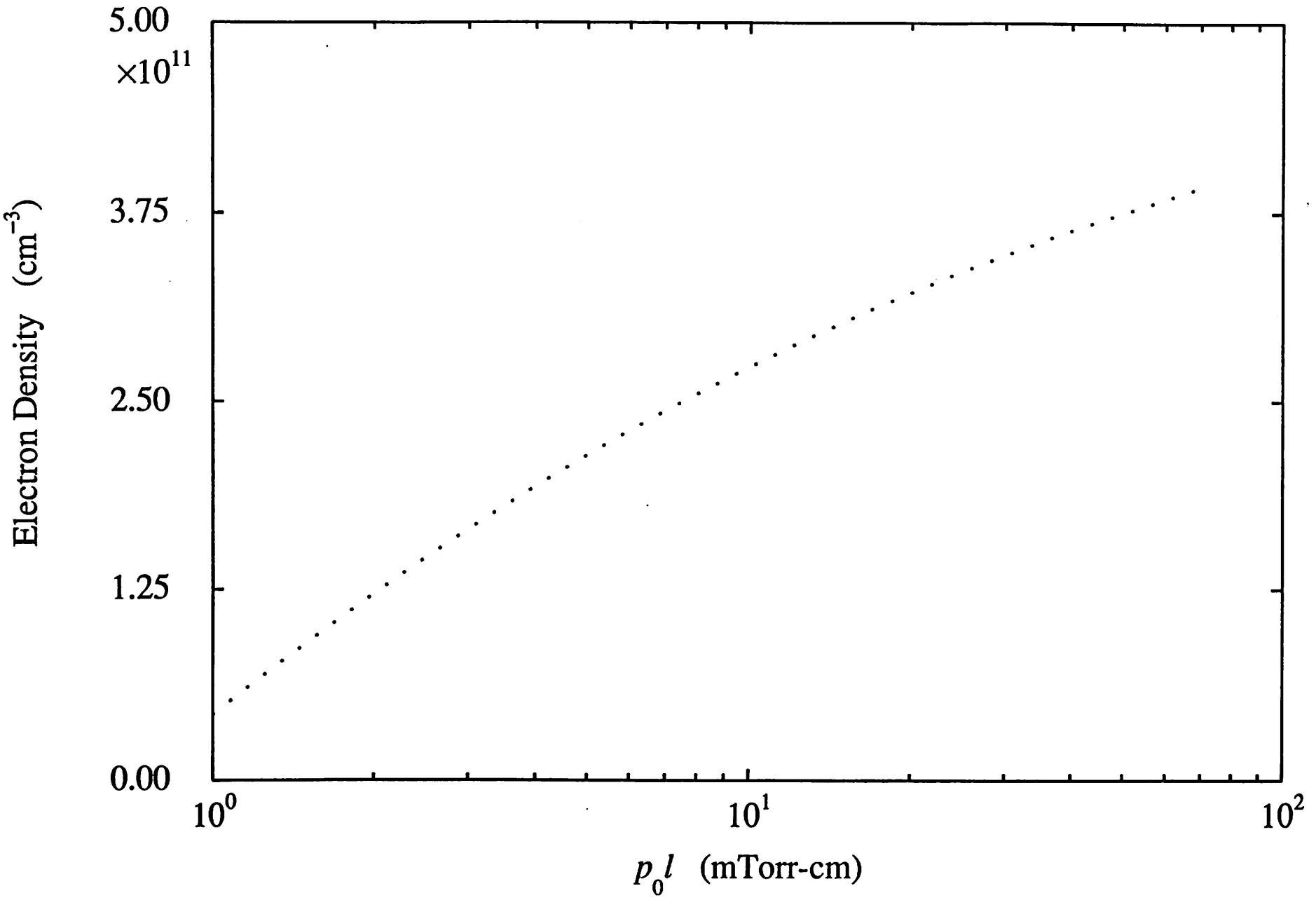
5.00
×10^11
3.75
2.50
1.25
0.00
Electron Density (cm^-3)
10^0
10^1
10^2
p_0 l (mTorr-cm)

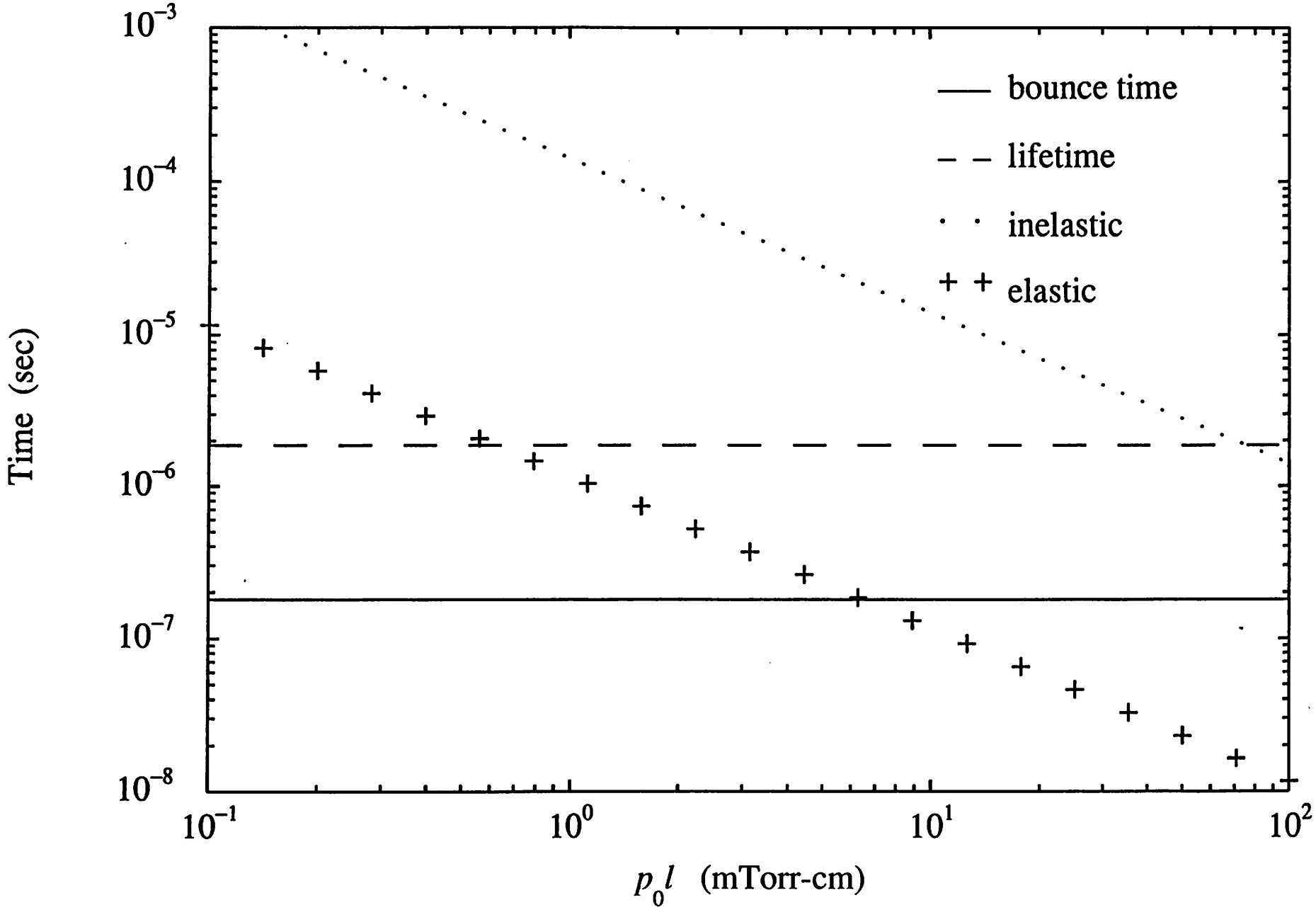
10^{-3}
10^{-4}
10^{-5}
10^{-6}
10^{-7}
10^{-8}
Time (sec)
bounce time
lifetime
inelastic
elastic
10^{-1}
10^{0}
10^{1}
10^{2}
$p_0 l$ (mTorr-cm)

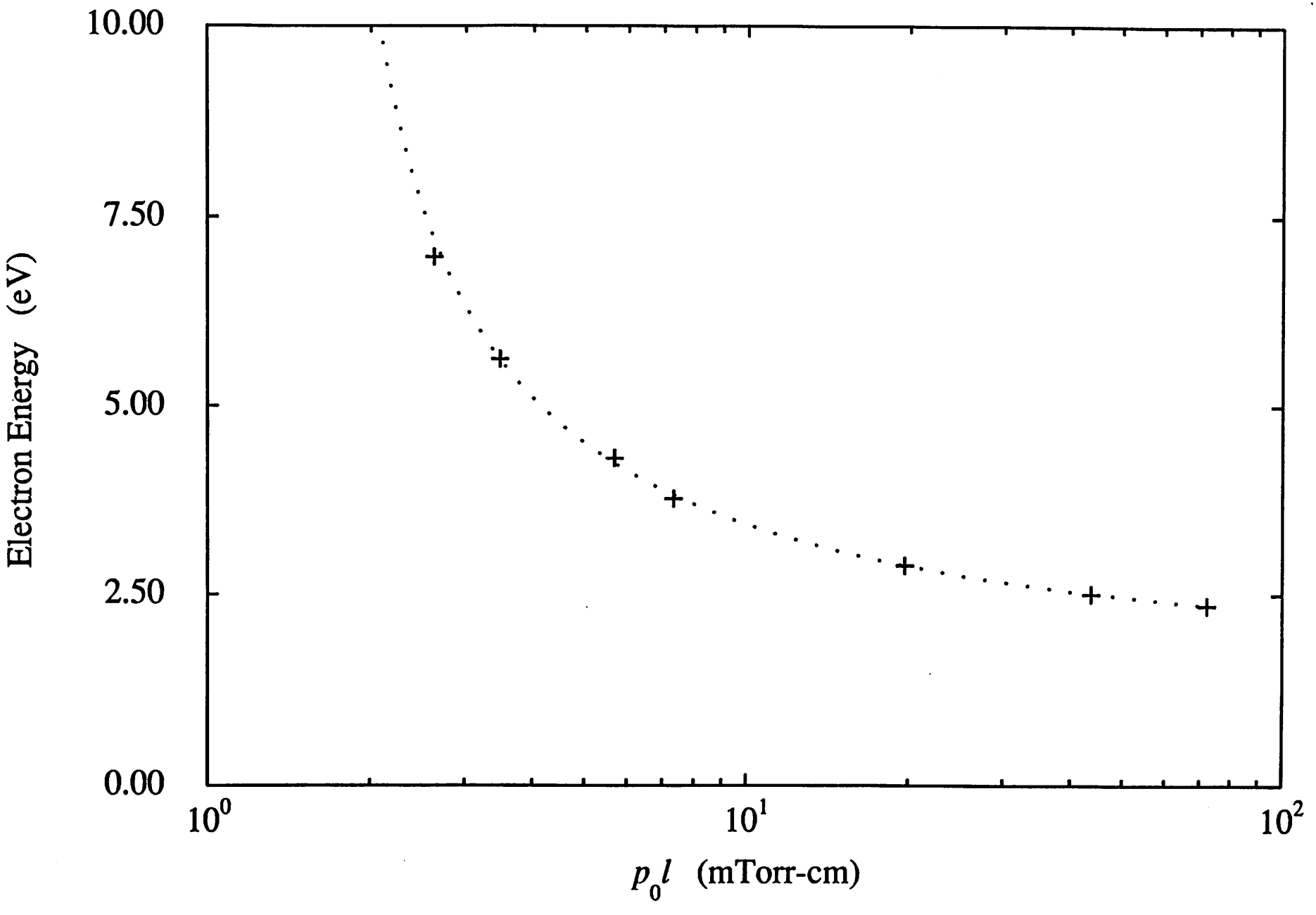
10.00
7.50
5.00
2.50
0.00
Electron Energy (eV)
10^0
10^1
10^2
$p_0 l$ (mTorr-cm)

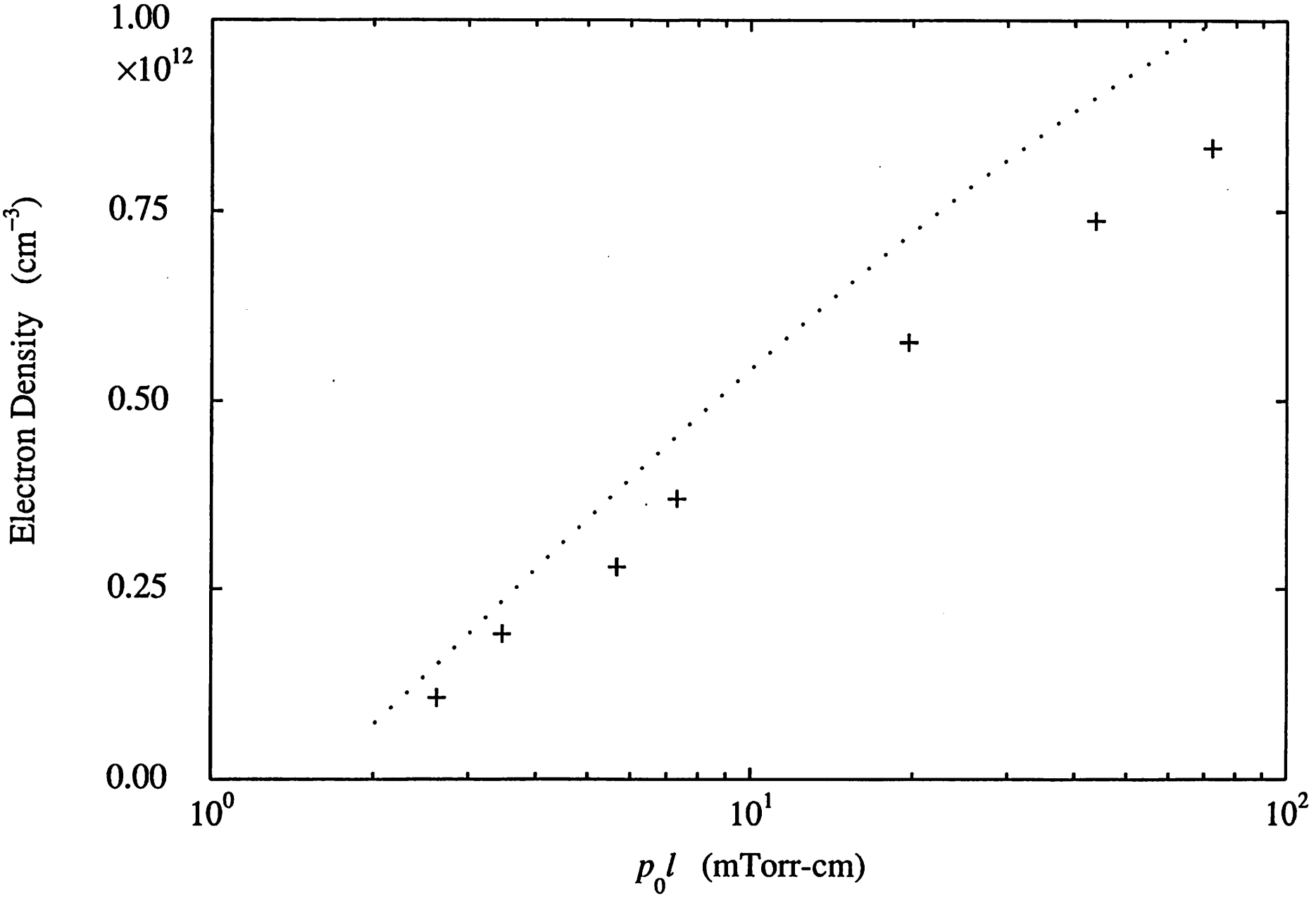
1.00
×10^12
0.75
0.50
0.25
0.00
Electron Density (cm^-3)
10^0
10^1
10^2
p_0 l (mTorr-cm)